

## Characteristics of Plasma Spraying Torch with a Hollow Cathode

LIN Lie (林烈), WANG Bo-yi (王柏一), WU Cheng-kang (吴承康)

Institute of Mechanics, the Chinese Academy of Sciences, Beijing 100080, China

**Abstract** A kind of plasma spraying torch with a hollow cathode is described in this paper. The plasma torch can be used for axial powder injection in plasma spray studies. The arc characteristics of the plasma torch with various gas flowrates, different gas media, are presented. The mathematical modeling and computational method are developed for predicting the temperature and velocity field inside the plasma torch.

**PACS:** 52.65, 52.30

### 1. Introduction

Plasma spraying has become a well-established and widely-used technology with various industrial applications[1,2,3]. In traditional plasma spraying, the design of plasma torch has been essentially the same, based on producing a plasma jet by a dc arc operated between a stick-type cathode and a nozzle-shaped anode[4,5]. The powder is injected radially into the plasma flame either within the anode channel or a short distance from the anode. With radial injection of powders the heating and dispersion of the injected powder is strongly dependent on the trajectory of the powder into the plasma jet. For different powders these trajectories are determined by particle size, density and injection velocity, and the range of trajectories is dependent on the size distribution of the powders being injected. So in the traditional plasma spraying torch the larger particles tend to pass through the plasma while the smaller particles tend to bounce off. This effect can be minimized with axially injecting torches, in which powders are injected in the center of the cathode. This type of

plasma spraying torch with a hollow cathode for axial powder feeding has been developed in our laboratory[6,7]. In this configuration, powders can follow a nearly-optimum trajectory with little or no segregation. This promotes high deposition rates and deposition efficiencies.

### 2. Plasma spraying torch with hollow cathode and its characteristics

The plasma spraying torch with a hollow cathode for axial powder feeding is shown schematically in Fig. 1. The cathode is made of a piece of ceria-tungsten with a cavity. The anode is made of copper. A narrow passage between the cathode and the anode provides a tangential inlet gas flow  $q_1$ . Another gas flow  $q_2$  and the powders are passed through the cavity of the hollow cathode into the region of arc column. The particles injected are progressively heated in the arc column before exiting the nozzle with plasma jet. Fig. 2 shows the photograph of plasma flame of the torch with hollow cathode.

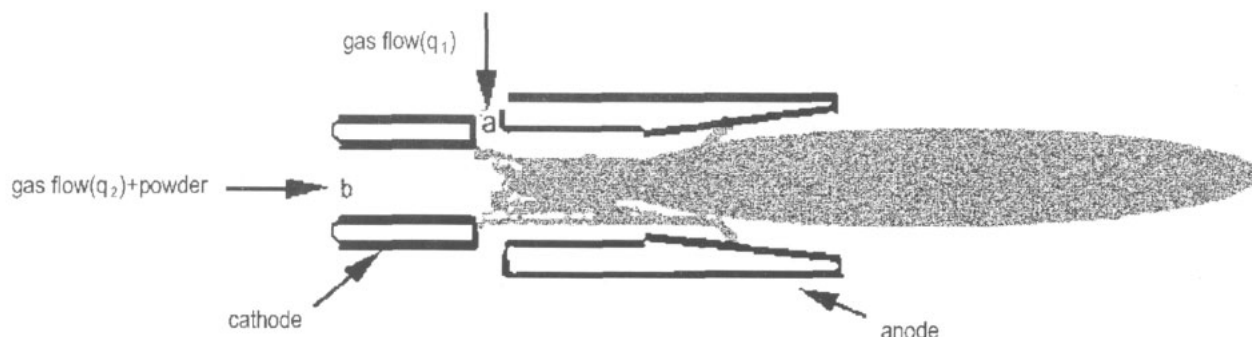


Fig.1 plasma spraying torch with a hollow cathode.

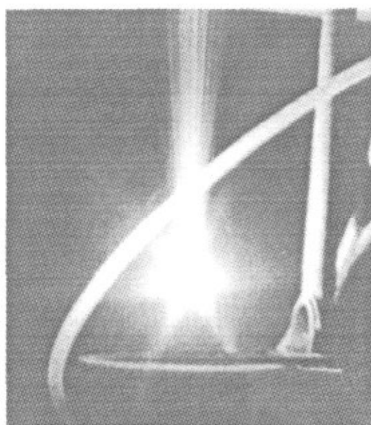


Fig.2 The photograph of plasma flame of the torch with hollow cathode.

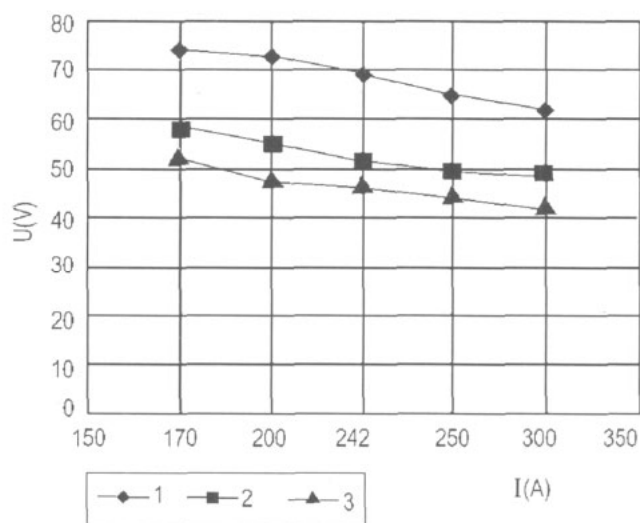


Fig.3 V-I characteristics of the plasma torch.

- 1  $q_1 = 1500 \text{ L/h}$  ,  $q_2 = 0$ ,  $\text{N}_2$
- 2  $q_1 = 1300 \text{ L/h}$  ,  $q_2 = 100 \text{ L/h}$ ,  $\text{N}_2$
- 3  $q_1 = 1500 \text{ L/h}$ ,  $q_2 = 0$ ,  $\text{Ar}$ .

Fig. 3 shows the volt-ampere characteristics of the plasma torch with hollow cathode under various conditions. In Fig. 3, the curve 1 ( $q_2 = 0$ ) and curve 2 ( $q_2 = 100 \text{ L/h}$ ) are the volt-ampere characteristics of the plasma torch for  $\text{N}_2$  , the curve 3 is the volt-ampere characteristics of the plasma torch for  $\text{Ar}$ . In Fig. 3, we can see that the curve 2 is lower than the curve 1. The reason is that when  $q_2 = 0$ , the arc root is inside the cavity of the hollow cathode , so the volts of the arc is higher than that when  $q_2 > 0$ .

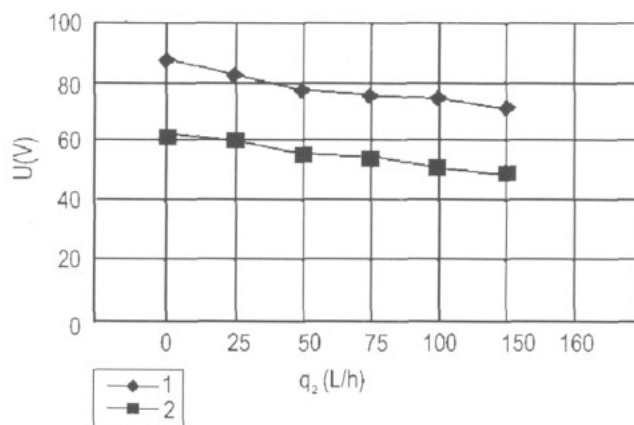


Fig.4 The relationship between  $q_2$  and  $U$ .

- 1  $q_1 = 1500 \text{ L/h}$ ,  $I = 200 \text{ A}$ ,  $\text{N}_2$
- 2  $q_1 = 1800 \text{ L/h}$ ,  $I = 220 \text{ A}$ ,  $\text{Ar}$

Fig. 4 shows the relationship between the gas flowrate  $q_2$  in the cavity of the hollow cathode and the arc voltage  $U$ . For the same gas flowrate  $q_1$  and arc ampere  $I$ , the arc voltage decreases with the increase in the gas flowrate  $q_2$ .

### 3. Calculation of the gas flowfield

The flowfield inside the torch has been calculated. The mathematical model is based on the solutions of appropriate conservation equations which describe the fluid- dynamical behavior of the plasma moving inside the torch. The basic assumptions made in our analysis are as follows: (1) The plasma torch is an axisymmetric system operating in a steady state; (2) The plasma is an optically-thin gas in local thermodynamic equilibrium; (3) The flow is laminar and compressible one with negligible buoyance and gravity effects; (4) The concept of equivalent heat source is adopted for the arc flow interaction, neglecting the details of the electromagnetic fields.

Modelling equations:

Due to swirling, the main gas has three velocity components in the axial, radial and azimuthal directions ( $u, v, w$ ) and three dimensional Navier-Stokes equations are presented in the cylindrical coordinates ( $z, \theta, r$ ):

$$\frac{\partial}{\partial z}(\rho u) + \frac{1}{r} \frac{\partial}{\partial r}(r \rho v) = 0, \quad (1)$$

$$\begin{aligned} & \frac{\partial}{\partial z}(\rho u v) + \frac{1}{r} \frac{\partial}{\partial r}(r \rho v u) \\ &= -\frac{\partial p}{\partial z} + 2 \frac{\partial}{\partial z} \left( \mu \frac{\partial u}{\partial z} \right) + \frac{1}{r} \frac{\partial}{\partial r} \left[ r \mu \left( \frac{\partial u}{\partial r} + \frac{\partial v}{\partial z} \right) \right], \end{aligned} \quad (2)$$

$$\begin{aligned} & \frac{\partial}{\partial z}(\rho u v) + \frac{1}{r} \frac{\partial}{\partial r}(r \rho v u) \\ &= -\frac{\partial p}{\partial r} + \frac{\partial}{\partial z} \left[ \mu \left( \frac{\partial v}{\partial z} + \frac{\partial u}{\partial r} \right) \right] \end{aligned}$$

$$+ \frac{2}{r} \frac{\partial}{\partial r} \left( r \mu \frac{\partial v}{\partial r} \right) - \mu \frac{2v}{r^2} + \rho \frac{\omega^2}{r}, \quad (3)$$

$$\begin{aligned} & \frac{\partial}{\partial z}[\rho u(r\omega)] + \frac{1}{r} \frac{\partial}{\partial r}[r \rho v(r\omega)] \\ &= \frac{\partial}{\partial r} \left[ \mu \frac{\partial(r\omega)}{\partial z} \right] + \frac{1}{r} \frac{\partial}{\partial r} \left[ r \mu \frac{\partial(r\omega)}{\partial r} \right] - \frac{2}{r} \frac{\partial}{\partial r}[\mu(r\omega)], \end{aligned} \quad (4)$$

$$\begin{aligned} & \frac{\partial}{\partial z}(\rho u h) + \frac{1}{r} \frac{\partial}{\partial r}(r \rho v h) \\ &= \frac{\partial}{\partial z} \left( \frac{k}{c_p} \frac{\partial h}{\partial z} \right) + \frac{1}{r} \frac{\partial}{\partial r} \left( \frac{r k}{c_p} \frac{\partial h}{\partial r} \right) + S_{arc} - S_R, \end{aligned} \quad (5)$$

where  $p$ ,  $\rho$  and  $h$  are the pressure, density and enthalpy respectively;  $\mu$ ,  $k$  and  $c_p$  are the viscosity, thermal conductivity and specific heat at constant pressure respectively;  $S_{arc}$  and  $S_R$  are the source terms accounting for arc heating and radiative loss respectively.

The governing equations (1)~(5) are numerically solved by using the finite difference scheme. The boundary conditions can be specific based on the geometry, size and operation parameters of our small-scale experimental facility. In the case without  $q_2$ , at the point b (see Fig. 1),  $u=0$ ,  $v=0$ ,  $\omega=0$ , and at the point a, the velocities were determined by measurement. In the case with  $q_2$ , at the point b,  $u=0$ ,  $v=0$ ,  $\omega$  was determined by measurement, and at the point a, the velocities were determined by measurement. The source by Joule heating induced the gas flow in three sections (radial cathode section, radial anode section and axial central section), the position of the arc root was determined by the experiment. The computations have employed an adaptation of the PHOENICS computing program. The computational domain is divided into an unequally spaced mesh of  $45 \times 120$  points. Staggered grids are used in order to overcome the difficulty in calculation of the velocity field due to the unknown pressure field. The converged solution can be arrived by the iteration procedure.

Numerical calculations are performed for the typical operation conditions: the inner diameter of the anode is 6 mm; the anode length is 40 mm; the cath-

ode cavity diameter is 6 mm; the cathode length is 12 mm; the current  $I=200$  A; the voltage  $U=85$  V; the flow rate of main gas  $q_1=1300$  L/h ( $w/v=10$ ) and the flow rate of auxiliary gas  $q_2=100$  L/h. Both the working and carrier gas are nitrogen in our system. The two cases with and without carrier gas respectively are considered in order to show the effect of auxiliary gas on the plasma flowfields.

It can be seen from Fig. 5 that the main gas injected from the sidewall entrance mainly discharges downstream but the injected gas near the cathode side deflects first upstream and then turns down-

stream in the axial direction. This deflection effect is the mechanism of driving the cathode arc root into the cavity. For the case without auxiliary gas, two large opposite vortices in the cathode cavity are induced by the working gas stream. However, a small amount of auxiliary gas can result in significant change in the cathode-cavity flowfield. The auxiliary gas injected axially from the endwall inlet leads to the disappearance of induced vortices and the suppression of deflection effect (see Fig. 6). It should be pointed out that the vector magnitude is plotted in logarithm in Fig. 5 and Fig. 6

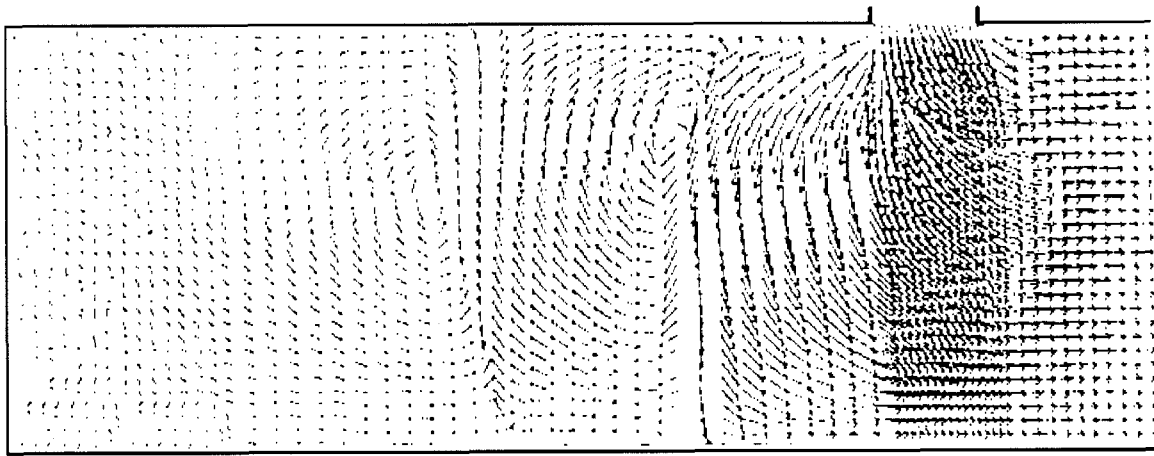


Fig.5 Velocity field in plasma torch without auxiliary gas.

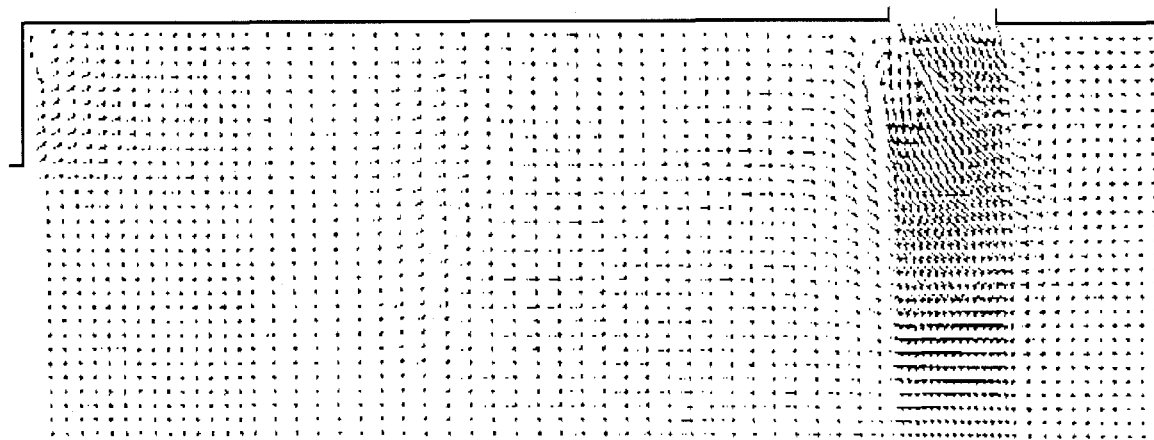


Fig.6 Velocity field in plasma torch with auxiliary gas.

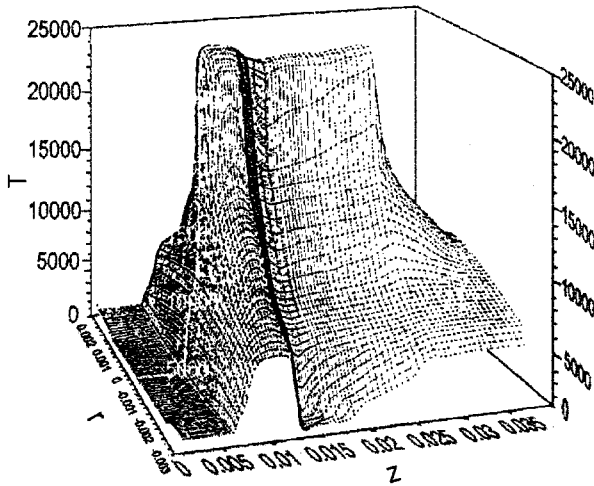


Fig.7 Temperature field in plasma torch without auxiliary gas.

As to the temperature field inside the plasma torch without auxiliary gas, it is shown in Fig. 7 that there are three different regions: (1) Low-temperature region ( $T < 3000$  K) near the main gas entrance ; (2) Medium-temperature ( $T = 3000 \sim 10000$  K) in the radial anode section of the arc column; (3) High-temperature region ( $T > 10000$  K) in the radial cathode section and axial central section of the arc column. The introduction of auxiliary gas results in the formation of cold region in front of the radial cathode section of the arc column (see Fig. 8). In this hot operation mode, the temperature gradient in the cathode-arc- root region is much higher than that in the anode-arc-region.

#### 4. Conclusions

A kind of plasma spraying torch with a hollow cathode for axial powder injection has been developed. The results of experimental research and numerical calculation are presented for this kind of plasma torch. The results show that the plasma torch can greatly improve plasma-heating efficiency and offer good prospect for the application in plasma spraying.

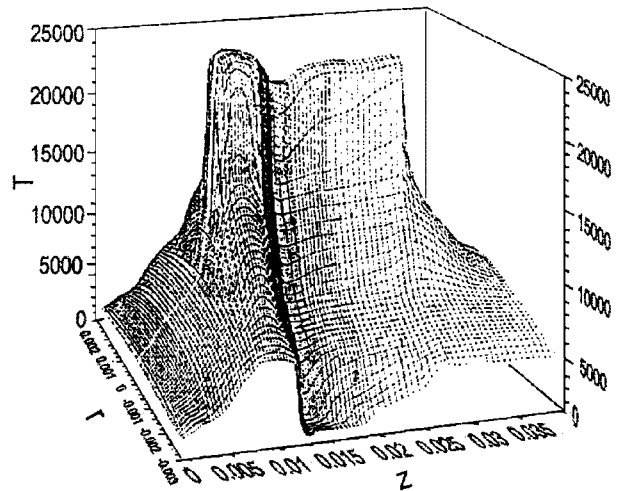


Fig.8 Temperature field in plasma torch with auxiliary gas.

#### Acknowledgment

The financial support from Beijing Aeronautical Manufacturing Technology Research Institute is gratefully acknowledged. (99JS50.3.2.ZK0402)

#### References

- [1] WU Hong-chen, YANG Xiang-dong, Characteristics of Laminar Plasma Jet and Process for spraying WC/Co Coating, ISPC-13, Beijing (1997) 1451-1454.
- [2] A.J.Farmer, N. Gane, S. Gulizia and R. Sekel, Plasma Spraying of Hydroxyapatite, SPC-13, Beijing(1997) 1434-1438.
- [3] D.Matejka, B. Benko, Plasma Spraying of Metallic and Ceramic Materials, Published by John Wiley & Sons Ltd., U.K (1989).
- [4] E. Pfender, Thermal Plasma Technology: Where Do We Stand and Where Are We Going", Plasma Chemistry and Plasma Processing 19(1) (1999)1-31.
- [5] Ph. Roumihac, J.F. Coudert, P. Fauchais, Designing Parameters of Spraying Plasma Torches, Thermal Spray Research and Applications, Proceeding of the Third National Thermal Spray Conference, Long Beach, CA, USA (1990)11-19.

- [6] WANG B.Y., LIN L., SUN Z., ZHAO Z. P., Flow-field Calculation of a Hollow-Thermionic-Cathode Reactor ISPC-13, Beijing (1997) 344-349. (Manuscript received 10 December 2000)
- [7] LIN L., SUN Z., WANG B.Y., WU C.K., A Thermionic Cathode with Diffused Arc Root for plasma Generator, ISPC-12, Minneapolis, USA (1995) 1437-1442.